wavevectors on one sheet correspond to scattering with phonon emission and on the other sheet to phonon absorption. For $\beta > 1$, the conic section is an ellipsoid with P at one focus. Scattering now occurs either by emission or by absorption, but not by both together (Fig. 7.4.2.3).

To evaluate the TDS correction, with **q** restricted to lie along the scattering surfaces, separate treatments are required for faster-than-sound ($\beta < 1$) and for slower-than-sound ($\beta > 1$) neutrons. The final results can be summarized as follows (Willis, 1970; Cooper, 1971):

(*a*) For faster-than-sound neutrons, the TDS rises to a maximum, just as for X-rays, and the correction factor is given by (7.4.2.13), which applies to the X-ray case. (This is a remarkable result in view of the marked difference in the one-phonon scattering surfaces for X-rays and neutrons.)

(*b*) For slower-than-sound neutrons, the correction factor depends on the velocity (wavelength) of the neutrons and is more difficult to evaluate than in (*a*). However, α will always be less than that calculated for X-rays of the same wavelength, and under certain conditions the TDS does not rise to a maximum at all so that α is then zero.

The sharp distinction between cases (*a*) and (*b*) has been confirmed experimentally using the neutron Laue technique on single-crystal silicon (Willis, Carlile & Ward, 1986).

7.4.2.4. *Correction factor for powders*

Thermal diffuse scattering in X-ray powder-diffraction patterns produces a non-uniform background that peaks sharply at the positions of the Bragg reflections, as in the single-crystal case (see Fig. 7.4.2.4). For a given value of the scattering vector, the one-phonon TDS is contributed by all those wavevectors **q** joining the reciprocal-lattice point and any point on the surface of a sphere of radius $2\sin\theta/\lambda$ with its centre at the origin of reciprocal space. These **q** vectors reach the boundary of the Brillouin zone and are not restricted to those in the neighbourhood of the reciprocal-lattice point. To calculate α properly, we require a knowledge, therefore, of the lattice dynamics of the crystal and not just its elastic properties. This is one reason why relatively little progress has been made in calculating the X-ray correction factor for powders.

7.4.3. Compton scattering
(By N. G. Alexandropoulos and M. J. Cooper)

7.4.3.1. *Introduction*

In many diffraction studies, it is necessary to correct the intensities of the Bragg peaks for a variety of inelastic scattering processes. Compton scattering is only one of the incoherent processes although the term is often used loosely to include plasmon, Raman, and resonant Raman scattering, all of which may occur in addition to the more familiar fluorescence radiation and thermal diffuse scattering. The various interactions are summarized schematically in Fig. 7.4.3.1, where the dominance of each interaction is characterized by the energy and momentum transfer and the relevant binding energy.

With the exception of thermal diffuse scattering, which is known to peak at the reciprocal-lattice points, the incoherent background varies smoothly through reciprocal space. It can be removed with a linear interpolation under the sharp Bragg peaks and without any energy analysis. On the other hand, in non-crystalline material, the elastic scattering is also diffused throughout reciprocal space; the point-by-point correction is consequently larger and without energy analysis it cannot be made empirically; it must be calculated. These calculations are imprecise except in the situations where Compton scattering is the dominant process. For this to be the case, there must be an encounter, conserving energy and momentum, between the incoming photon and an individual target electron. This in turn will occur if the energy lost by the photon, $\Delta E = E_1 - E_1$, clearly exceeds the one-electron binding energy, E_B, of the target electron. Eisenberger & Platzman (1970) have shown that this binary encounter model – alternatively known as the impulse approximation – fails as $(E_B/\Delta E)^2$.

Table 7.4.3.1. *The energy transfer, in eV, in the Compton scattering process for selected X-ray energies*

Scattering angle φ (°)	Cr $K\alpha$ 5411 eV	Cu $K\alpha$ 8040 eV	Mo $K\alpha$ 17 443 eV	Ag $K\alpha$ 22 104 eV
0	0	0	0	0
30	8	17	79	127
60	29	63	292	467
90	57	124	575	915
120	85	185	849	1344
150	105	229	1043	1648
180	112	245	1113	1757

Data calculated from equation (7.4.3.1).

The likelihood of this failure can be predicted from the Compton shift formula, which for scattering through an angle φ can be written.

$$\Delta E = E_1 - E_2 = \frac{E_1^2(1-\cos\varphi)}{mc^2[1+(E_1/mc^2)(1-\cos\varphi)]}. \qquad (7.4.3.1)$$

This energy transfer is given as a function of the scattering angle in Table 7.4.3.1 for a set of characteristic X-ray energies; it ranges from a few eV for Cr $K\alpha$ X-radiation at small angles, up to ~ 2 keV for backscattered Ag $K\alpha$ X-radiation. Clearly, in the majority of typical experiments Compton scattering will be inhibited from all but the valence electrons.

7.4.3.2. *Non-relativistic calculations of the incoherent scattering cross section*

7.4.3.2.1. *Semi-classical radiation theory*

For weak scattering, treated within the Born approximation, the incoherent scattering cross section, $(\mathrm{d}\sigma/\mathrm{d}\Omega)_{\mathrm{inc}}$, can be factorized as follows:

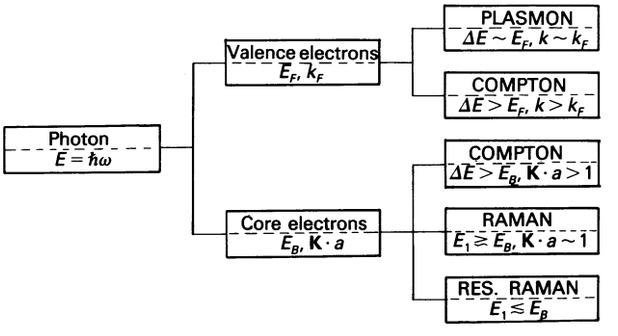

Fig. 7.4.3.1. Schematic diagram of the inelastic scattering interactions, $\Delta E = E_1 - E_2$ is the energy transferred from the photon and **K** the momentum transfer. The valence electrons are characterized by the Fermi energy, E_F, and momentum, k_F ($\hbar$ being taken as unity). The core electrons are characterized by their binding energy E_B. The dipole approximation is valid when $|\mathbf{K}|a < 1$, where a is the orbital radius of the scattering electron.

references